applied sciences

MDPI

Article

β-Phosphonated Glycine Pendant Groups Grafted on Styrene-6.7% Divinylbenzene Copolymers: Synthesis and Their Application as Photocatalysts

Adriana Popa [1], Laura Cocheci [2,*], Lavinia Lupa [2], Aniela Pop [2] and Aurelia Visa [1]

[1] "Coriolan Dragulescu" Institute of Chemistry, 24 Mihai Viteazul Blv., 300223 Timisoara, Romania
[2] Faculty of Industrial Chemistry and Environmental Engineering, Politehnica University Timisoara, 6 Vasile Parvan Blv., 300223 Timisoara, Romania
* Correspondence: laura.cocheci@upt.ro

Featured Application: The synthesised and characterised novel compounds of β-phosphonate-type glycine pendant groups grafted on S-DVB copolymer present a great potential application in the treatment of water with organic pollutants, such as effluents resulting from the pharmaceutical, food or textile industry.

Abstract: Environmental pollution from organic contaminants caused by textile dyeing is a real danger. Wastewater from the textile industry has high organic loads, as well as dyes and chemical compounds used in their preparation. Among the azo dyes, Congo red (CR) dye is widely used as a model in the experimental studies of textile wastewater treatment. Heterogeneous photocatalysis consists of UV or VIS light irradiation of various types of organic compounds in water in the presence of a solid catalyst; it is considered an important technique for the purification and reuse of aqueous effluents. In the present study, two novel compounds of β-phosphonate-type glycine pendant groups grafted on S-DVB copolymer were used for the decontamination of Congo red dye polluted water. They were characterized by FTIR spectroscopy, scanning electron microscopy, EDX spectroscopy, thermogravimetric analysis and UV-VIS spectroscopy. By using 25 mg/L initial concentration of Congo red dye and a catalyst concentration of 1 g/L and 240 min of irradiation, a photocatalysis efficiency of 98.6% in the case of [(diethyl)(phosphono)methylene]glycine pendant groups grafted on styrene-6.7% divinylbenzene copolymer (EthylAmAcid material), and of 83.1% in the case of [(dibenzyl)(phosphono)methylene]glycine pendant groups grafted on styrene-6.7% divinylbenzene copolymer (BenzylAmAcid material), respectively, was achieved.

Keywords: grafted copolymers; synthesis; photocatalysis

Citation: Popa, A.; Cocheci, L.; Lupa, L.; Pop, A.; Visa, A. β-Phosphonated Glycine Pendant Groups Grafted on Styrene-6.7% Divinylbenzene Copolymers: Synthesis and Their Application as Photocatalysts. *Appl. Sci.* **2023**, *13*, 2025. https://doi.org/10.3390/app13032025

Academic Editor: Domenico Lombardo

Received: 23 December 2022
Revised: 19 January 2023
Accepted: 31 January 2023
Published: 3 February 2023

1. Introduction

Textile wastewater pollution control requires great attention to solve the problem of discharging wastewater directly into the environment in order to reduce the ecotoxicological effect of dyes. Moreover, there is the possibility of reusing process water and chemicals [1]. Due to their intense utilization, organic dyes are currently considered as micropollutants [2]. Because they are found in low concentrations in the aquatic medium [3] and due to their poor biodegradability, they are practically considered to be ubiquitous in the environment, making the efforts to remove them from textile wastewater increase more and more.

The treatment processes of wastewater containing organic dyes are physico-chemical (sedimentation, filtration, flotation, coagulation, adsorption, membrane separation and incineration), chemical (neutralization, oxidation, reduction and electrolysis) and biological (aerobic or anaerobic) [4–6]. In general, the treatment scheme for the wastewater from the texile industry has three stages: pretreatment (fine straining, sedimentation and neutralization), biological treatment with activated sludge and tertiary treatment

(coagulation-flocculation, adsorption, membrane separation, oxidation and electrolysis). Among these, the adsorption and advanced oxidation processes have proven to have good results in the tertiary treatment process of the effluents from the textile industry. While adsorption concentrates the compound onto the surface of the adsorbent material followed by its separation from water [7,8], the advanced oxidation processes result in the oxidative degradation of the compounds, respectively, and their complete removal from the aqueous environment. The advanced oxidation process implies the generation of strong oxidizing species (hydroxyl radicals or radicals based on sulphate or chlorine species) in the reaction medium to oxidize organic compounds. Among the advanced oxidation processes, we can mention the following: homogeneous ultraviolet irradiation (direct irradiation or photolytic oxidation mediated by hydrogen peroxide (UV/H_2O_2) and/or ozone ($UV/H_2O_2/O_3$ or UV/O_3)), heterogeneous photocatalysis, electron-beam irradiation, supercritical water oxidation, ultrasonic irradiation or electrohydraulic cavitation [9,10].

Heterogeneous photocatalysis can be defined as the initiation of an oxidation reaction under the action of UV, VIS or IR radiation in the presence of a solid material, called a photocatalyst, which absorbs these radiations and participates in the generation of the oxidizing species. After proving that TiO_2 is a very good photocatalyst, many solid materials have been developed to be used as photocatalysts, for example, titania based materials [11–13], zinc based materials [14], copper based materials [15], layered double hydroxides [16] and polymers [17–19]. The complex architecture of polymers allows, almost unlimitedly, the synthesis of new materials with tunable properties. The alternative to inorganic or inorganic–organic hybrid photocatalyzing materials could be a polymer with similar properties that is easier to synthesize. Functionalization of polymeric supports with pendant active groups has yielded structures with improved properties that can be used in a wide range of applications. The use of polymers composite presents an increase in the water treatment technology's performance due to the synergic effect brought about by the support and functional groups. In previous studies, as a functional group was introduced aminophosphonate groups on styrene-divinylbenzene supports, which were tested as adsorbents [20]. The functionalized polymers immobilized with transitional metals by coordination were studied as catalysts in the oxidation process of organic compounds with hydrogen peroxide [21]. In order to protect the environment, current trends are considering the possibilities of using the polymeric materials as supports with active pendant groups that could play an important role in the decontamination of aqueous systems and the recovery of toxic substances. A new functional group was studied, β-phosphonate glycine groups, for the functionalization of the styrene-6.7% divinylbenzene copolymer, and the obtained composite polymer was used for the first time as a photocatalyst in the water treatment process. From the literature survey, there are no published studies on using this type of functionalized polymer in the photocatalytic treatment process of water with dyes content.

The objective of the present study is the synthesis, characterization and use as photocatalysts of two polymeric materials obtained by grafting on styrene-divinylbenzene copolymer of the β-phosphonate-type glycine pendant groups.

The goal of the functionalization of copolymers with β-phosphonate glycine groups is to improve their adsorption/catalytic properties towards specific organic compounds present in the wastewater. The obtained copolymer functionalized with β-phosphonate glycine groups were characterized by FTIR spectroscopy, termogravimetric analysis, SEM/EDX analysis. In this study, polymeric heterogeneous photocatalysts with β-phosphonate glycine groups were tested in dark adsorption studies, and kinetics studies in the photocatalysis of the azo Congo red (CR) dye from water. The influence of initial concentration of the dye and the catalyst amount, as well as the possibility of catalyst reuse were investigated. Obtaining modified copolymers with pendant groups that can be easily recovered and reutilized without any contamination of the environment was our main interest. We are reporting some new results that show that the two materials (EthylAmAcid and BenzylAmAcid)

can be successfully used in the Congo red dye removal from water through the process of heterogeneous photocatalysis.

2. Materials and Methods

2.1. Materials

Styrene-6.7% divinylbenzene copolymer functionalized with aldehyde groups (G_F = 2.80 mmoles aldehyde groups/g copolymer, synthesized in our laboratory [20]), an aminoacid (glicine), diethylphosphite, dibenzylphosphite and ethanol (Chimreactiv, p.a.) were used as starting materials for the preparation of the photocatalytic polymers. All other chemicals were used without further purification.

2.2. Obtaining of β-Phosphonated Glycine Pendant Groups Grafted on Styrene-6.7% Divinylbenzene Copolymers

7 g of styrene-6.7% divinylbenzene copolymer with aldehyde pendant groups was left in ethanol (100 mL) for 24 h to allow the copolymer beads to swell. Functionalization of the copolymers with glicine and diethylphosphite/dibenzylphosphite was carried out at molar ratios of 1:1:1 and at reflux for 30 h. Then, styrene-6.7% divinylbenzene copolymers functionalized with pendant groups (by type: [(diethyl)(phosphono)methylene]glycine (Code: EthylAmAcid) and [(diphenyl)(phosphono)methylene]glycine (Code: BenzylAmAcid)) were separated by filtration, washed with ethanol and dried at 50 °C for 24 h.

2.3. Application as Photocatalysts for Congo Red Dye Removal

The photocatalysis experiments were carried out in a PhotoLAB B400-700 Basic Batch-L-type photocatalytic reactor, purchased from Peschl-Ultraviolet GmbH, Mainz, Germany, equipped with a TQ150-type submerged lamp (150 W Hg medium pressure). The temperature of the system did not exceed 20 °C, due to the circulation of tap water in the outer mantle of the reactor. An amount of 700 cm^3 of CR solution (concentrations: 25, 50 and 100 mg/L) was magnetically stirred with a certain mass of photocatalyst, so that the catalyst amount was 0.5, 1 and 2 g/L. Preliminary dark adsorption experiments were carried out, in order to study the equilibrium time achieved between the surface of the photocatalyst and the dye. After this time, the lamp was turned on. At well-established time intervals, 5 mL aliquots were taken, filtered through a Millipore syringe filter (45 μm pore size) and spectrophotometrically analysed. The spectra were recorded between 200 and 800 nm and the maximum absorption values at λ = 498 nm were monitored. The Lambert–Beer's law was utilized to establish the relationship between absorption and CR concentration. The efficiency of the removal of CR was calculated by using the following equation:

$$\text{Efficiency}(\%) = \frac{c_0 - c}{c_0} \cdot 100, \quad (1)$$

where c_0 is the initial concentration of CR (mg/L) and c is the concentration of CR at time t (mg/L).

2.4. Characterization Methods

The FTIR spectra were carried out using a Jasco FTIR spectrophotometer in the range of 400–4000 cm^{-1}, using KBr pellets with a resolution of 4 cm^{-1}. Scanning electron microscopy (SEM) analysis and elemental analysis (EDX) were performed using a Quanta FEG 250 Microscope. Thermal properties were studied through thermogravimetric analysis (TG) using TGA/SDTA 851-LF1100-Mettler equipment at a heating rate of 10 °C/min under nitrogen atmosphere, and temperature in the range of 25–900 °C.

Diffuse reflectance spectra of polymers were measured by using a Varian Cary 100 UV-VIS spectrophotometer equipped with an integrating diffuse reflectance sphere. The band gap energies were deduced after measurements by using the Kubelka–Munk equation.

The CR solution concentrations were analysed from the UV-VIS spectra recorded by using the Varian Cary 100 spectrophotometer.

3. Results and Discussions

3.1. Samples Characterization

In the present study, through a facile one-pot strategy, [(diethyl)(phosphono) methylene]glycine pendant groups and [(diphenyl)(phosphono)methylene]glycine pendant groups grafted on styrene-6.7% divinylbenzene copolymers were prepared successfully using amino acid, diethylphosphite/dibenzylphosphite and aldehyde copolymers as matrix (see Scheme 1).

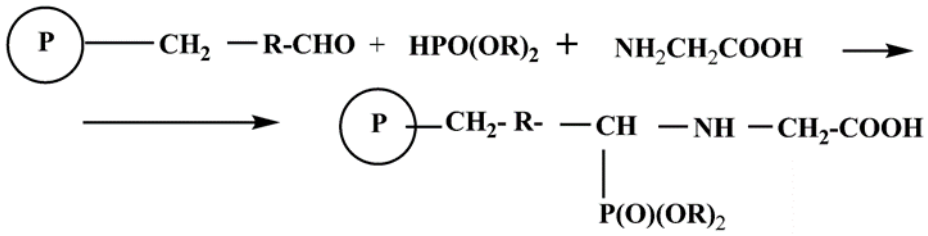

Scheme 1. Preparation of [(diethyl)(phosphono)methylene]glycine pendant groups/[(dibenzyl) (phosphono)methylene]glycine pendant groups grafted on styrene-6.7% divinylbenzene copolymer, where R = -O-C_6H_4-; R = Et:-ethyl, Bz:-benzyl (Code: EthylAmAcid/BenzylAmAcid).

Within the limits of inherent experimental errors, Table 1 present the results obtained in the characterization of the functionalized copolymers by determining the phosphorus and nitrogen content.

Table 1. EDX for [(diethyl)(phosphono)methylene] glycine pendant groups/[(dibenzyl)(phosphono) methylene]glycine pendant groups grafted on copolymer. (Code: EthylAmAcid/BenzylAmAcid.)

Elem./Wt%	EthylAmAcid Sample	BenzylAmAcid Sample
C	72.1	80.5
N	4.55	2.24
O	21.7	16.1
P	1.51	1.11
Cl	0.141	0.0103

In Figure 1a, it is seen that the beads exhibit as a perfect ball, with the diameter varying from 476 μm to 864 μm. In addition, in Figure 1b, it is seen that the sample has a rough surface and uniform distribution of pores.

The comparative interpretation of the IR spectra (Figure 2) for the synthesized samples (EthylAmAcid and BenzylAmAcid) and aldehyde support shows a decrease in the intensity of the aromatic aldehyde groups' absorption band at 1697 cm^{-1}, corresponding to C=O stretching at the aromatic nucleus, confirming that the reaction occurred at the aromatic aldehyde groups. It also shows a slight increase in the adsorption band intensity from 1592 cm^{-1}, indicating the presence of N-H valence vibrations, and shows that the aliphatic P-O-C stretch causes an increase in the intensity of the adsorption band at 1017 cm^{-1}.

The comparative interpretation of the TG spectra (Figure 3) for the synthesized sample (EthylAmAcid) and aldehyde support shows that after 900 °C, the decomposition of EthylAmAcid sample gives 19.3% residue; that after 900 °C, the aldehyde support shows better stability, and at decomposition it gives 34% residue; and that the EthylAmAcid sample has stability up to a temperature of 260 °C compared to aldehyde support, which is stable up to a temperature of 420 °C.

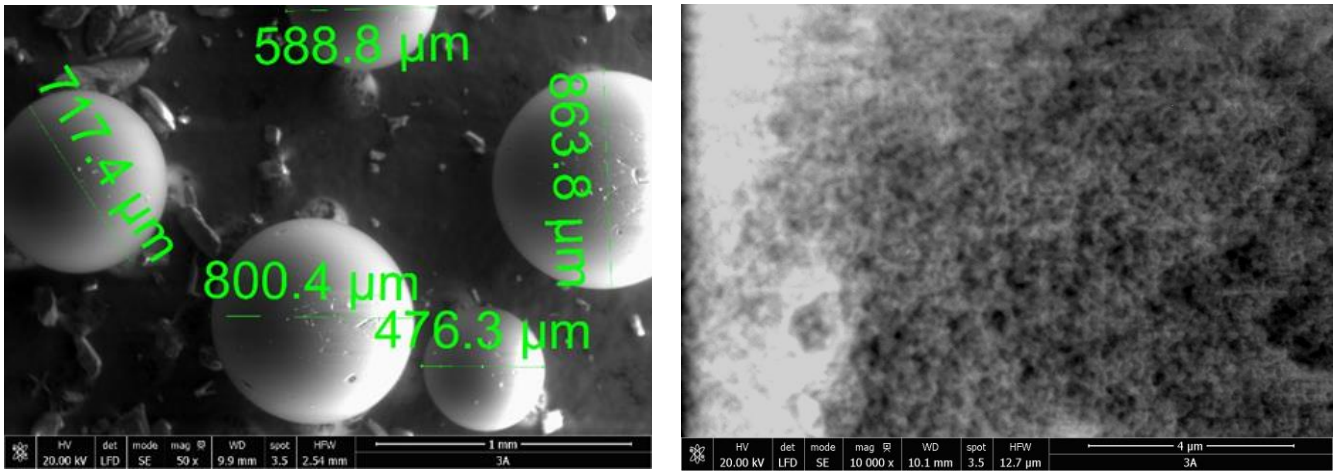

(**a**) (**b**)

Figure 1. SEM images for [(diethyl)(phosphono)methylene]glycine pendant groups grafted on copolymer (Code: EthylAmAcid): (**a**) polymer beads at 50× magnitude; (**b**) rough surface of a bead at 10,000× magnitude.

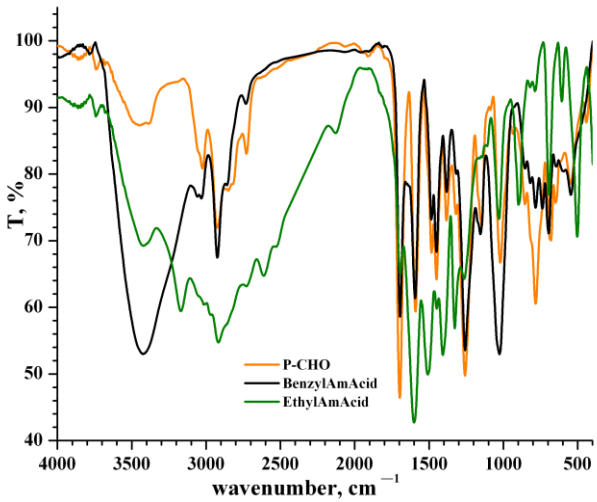

Figure 2. FTIR for EthylAmAcid, BenzylAmAcid samples and aldehyde support.

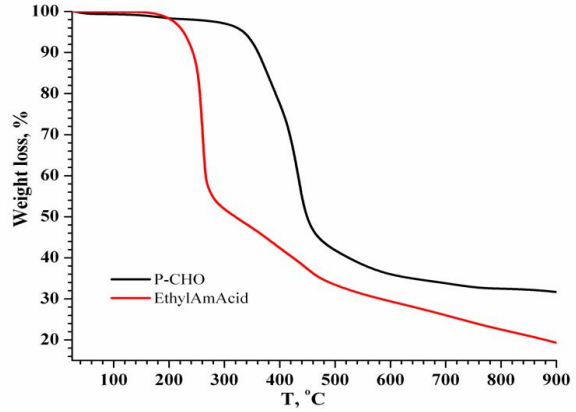

Figure 3. TG analysis for EthylAmAcid sample and aldehyde support.

Thus, upon the introduction by functionalization of β-phosphonate glycine pendant groups, the EthylAmAcid sample becomes less stable compared to the raw material.

The UV-VIS spectra for the samples are presented in Figure 4. The spectra present a broad absorption band in the UV domain, with two shoulders at 260 and 320 nm, that originate from the intra-aromatic π–π* transitions in copolymer [21]. The direct allowed band gap energies, calculated from the Kubelka–Munk transformed diffuse reflectance spectra, are 3.60 eV for EthylAmAcid sample and 3.65 eV for BenzylAmAcid sample. The values of band gap energies are in the domain of the energies calculated for other polymers [22,23]. The type of the groups, [(diethyl)(phosphono)methylene]glycine pendant groups or [(dibenzyl)(phosphono)methylene]glycine pendant groups, grafted on copolymer does not lead to obtaining very different values for the band gap energy. The small variation band gap energy for these structures may be due to the subtle difference in their structural arrangement. It is expected that the behavior of the samples will be similar in the process of heterogeneous photocatalysis.

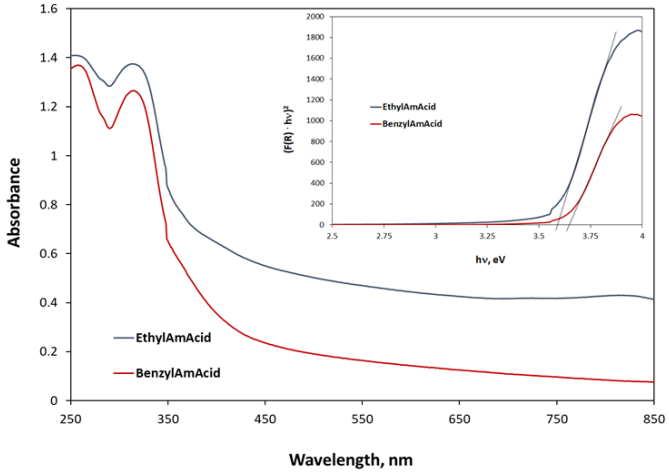

Figure 4. UV-VIS spectra of the synthetized samples. Inlet: Kubelka–Munk transformed function from diffuse reflectance spectra.

3.2. Photocatalysis for Congo Red Dye Removal

3.2.1. Dark Adsorption Studies

Adsorption capacity is an important characteristic of the solid photocatalysts because the generation of the oxidant species and the oxidation process of organic dye compounds takes place at the surface of the solid. On the one hand, a good adsorption capacity ensures the presence of the organic dye compound on the catalyst surface, where the oxidation process takes place [24]. The studies that have been carried out regarding the synergistic effect of adsorption and photocatalysis on the removal of dyes from the water have shown that the materials that have high adsorption capacities have higher removal efficiencies [24], but these performances depend especially on the affinity of the adsorbent material towards the organic compound. On the other hand, the use of adsorbent materials with high adsorption capacity does not economically justify the use of these materials as photocatalysts. In addition, a very high adsorption capacity prevents the radiation generated by the lamp from reaching the surface of the catalyst to initiate the process of generating electron-hole couples that give rise to oxidizing radicals. Studying the synergistic effect of adsorption and photocatalysis developed by carbon nitride-based composite nanosheets, it was concluded that a high adsorption efficiency is followed by a low photocatalysis efficiency [25].

The dark adsorption studies give also information about the time needed to achieve the equilibrium and about the extent of adsorption. The variation in the CR concentration across time when conducting the adsorption studies in the dark is shown in Figure 5. A sharp decrease in the CR concentration is observed in the first 5 min after the contact between the dye solution and the solid materials, then the concentration decreases more slowly, the equilibrium being reached after 30 min of contact.

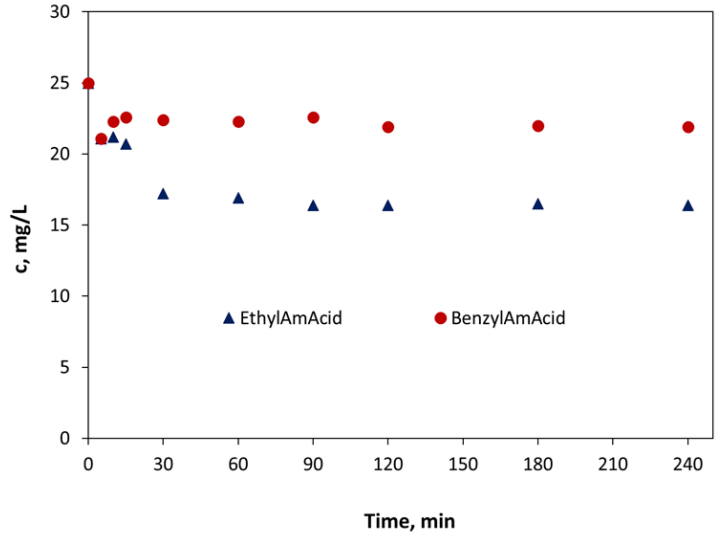

Figure 5. Variation in CR concentration versus time in dark adsorption. c_0 = 25 mg/L. Catalyst concentration = 1 g/L.

The adsorption efficiency developed by the two materials is: 34.4% for EthylAmAcid and 12.5% for BenzylAmAcid. Under these experimental conditions, the equilibrium adsorption capacities reached the values of 8.62 mg/g for EthylAmAcid and 1.95 mg/g for BenzylAmAcid, respectively.

The main application of polymers and composite polymers in water treatment, and especially in the tertiary treatment process of dye removal, is adsorption. A varied class of polymers and polymeric composites was synthesized, characterized, and tested for the study of their adsorbent performances. For example, a polyaniline-zinc titanate composite has proven an adsorption efficiency of over 95% in 15 min, when removing CR with an initial concentration of 50 mg/L [26]. A polystyrene/CuO/calcined layered double hydroxide composite has developed a maximum adsorption capacity of 485 mg/g, with an efficiency of over 95% in removing CR dye from water [27]. Comparing the adsorption efficiencies developed by other polymeric materials with those of the two studied materials, it can be concluded that their use as adsorbents is not economically feasible.

3.2.2. Efficiency of Photocatalysts

A comparison between the photocatalysis efficiency developed by the materials EthylAmAcid, BenzylAmAcid and P-CHO is presented in Figure 6. Starting from the initial concentration of 50 mg/L CR, the photolysis efficiency was 47.7% after 240 min of irradiation. Aldehyde support (sample P-CHO) has poor photocatalyst characteristics; after 240 min of reaction, a CR removal efficiency of 60.5% was achieved. However, samples EthylAmAcid and BenzylAmAcid have developed verry good efficiencies, of 95.3% and 85.1%, respectively. It can be concluded that by grafting the aldehyde support with the [(diethyl)(phosphono)methylene] glycine pendant groups/[(dibenzyl)(phosphono)methylene] glycine pendant groups, the photocatalyst characteristics of the synthesized materials are improved. The two studied materials (EthylAmAcid and BenzylAmAcid) presented a low adsorption capacity, but in the meantime developed a very good photocatalysis efficiency. These underline their efficiency to be used as catalytic materials in the degradation process of dyes from water using photocataysis treatment.

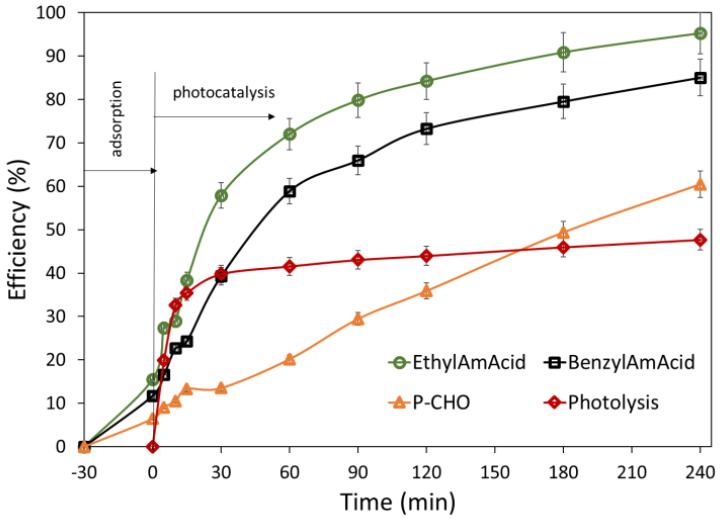

Figure 6. Photocatalysis efficiency. c_0 = 50 mg/L. Catalyst concentration = 1 g/L.

3.2.3. Influence of Congo Red Initial Concentration

The influence of the initial concentration of the dye is shown in Figure 7. At a lower initial concentration (of 25 mg/L), almost all the dye was removed from the solution after 240 min of heterogeneous photocatalysis, when using material EthylAmAcid as a catalyst (Figure 7a). The efficiency of CR removal was calculated, and it was 98.6%. With an increase in the initial concentration, the efficiency of the photocatalysis process decreases, reaching 86.0% for 100 mg/L CR. When we used material BenzylAmAcid as a photocatalyst, it can be seen from Figure 7b that the lower initial concentrations of CR had a weak influence on the efficiency of the process. The efficiency was 83.1% and 85.1% when starting from the initial concentration of 25 mg/L and 50 mg/L, respectively. For an initial CR concentration of 100 mg/L, and using material BenzylAmAcid as the photocatalyst, a process efficiency of 73.1% was obtained. The efficiency of CR dye removal from the solutions with different initial concentrations and using the two materials as photocatalysts are presented in Table 2.

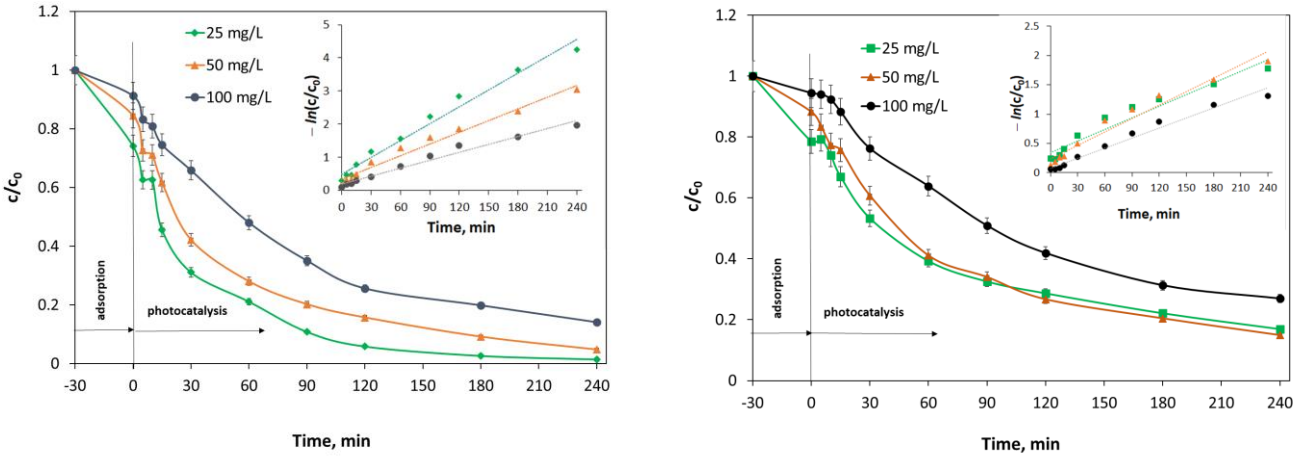

Figure 7. Influence of the initial concentration of CR when using EthylAmAcid as the photocatalyst (**a**); BenzylAmAcid as the photocatalyst. Inset: kinetics of photocatalysis (**b**). Solid catalyst amount = 1 g/L. Inset: kinetics of photocatalysis.

Table 2. CR removal in different conditions.

Material	c_0 (mg/L)	Solid:Liquid (g/L)	Efficiency (%)	$k_{app} \cdot 10^2$ (min^{-1})	R^2
EthylAmAcid	25	1	98.6	1.69	0.9796
	50	1	95.3	1.18	0.9771
	100	1	86.0	0.802	0.9737
	50	0.5	93.1	1.01	0.9774
	50	2	92.2	1.00	0.9608
BenzylAmAcid	25	1	83.1	0.661	0.9430
	50	1	85.1	0.761	0.9596
	100	1	73.1	0.569	0.9760
	50	0.5	81.2	0.533	0.9114
	50	2	92.7	1.09	0.9525

3.2.4. Influence of Solid Catalyst Amount

The amount of solid catalyst influences the efficiency of the photocatalysis process; the catalyst surface exposed to irradiation is higher if the solid:liquid ratio is higher. The influence of solid:liquid ratio is presented in Figure 8. By starting from a solution with 50 mg/L CR, and with material EthylAmAcid utilized as a photocatalyst, the efficiency of the dye removal process does not vary significantly with the catalyst amount. The best efficiency was obtained at the solid:liquid ratio of 1 g/L, being 95.3%. When using material BenzylAmAcid as a photocatalyst, the amount of 2 g/L proved to have the best efficiency (92.7%) on removing CR from the aqueous solution. The efficiencies achieved when using various quantities of solid catalyst, for the two materials, are presented in Table 2.

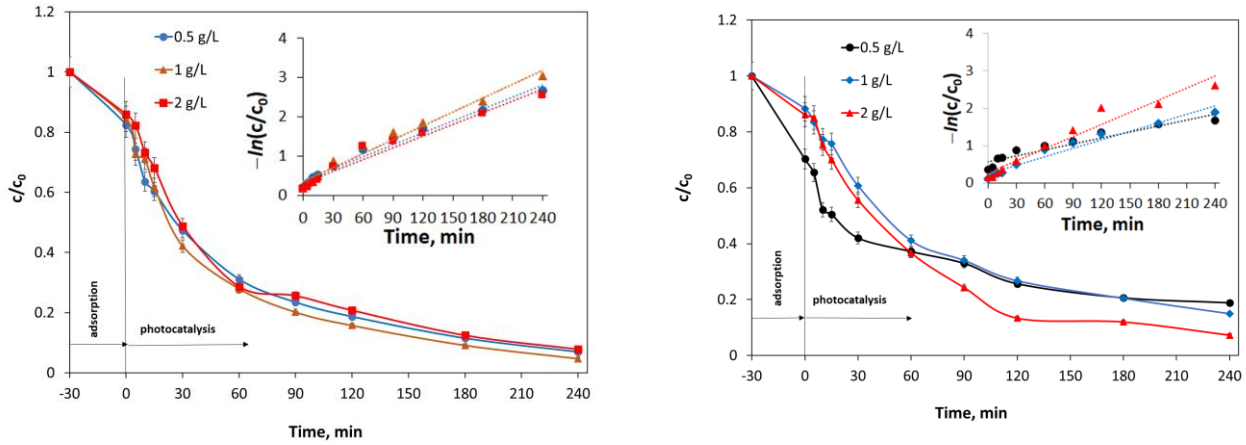

Figure 8. Influence of solid catalyst amount when using EthylAmAcid as the photocatalyst (**a**); BenzylAmAcid as the photocatalyst. Inset: kinetics of photocatalysis (**b**). c_0 = 50 mg/L. Inset: kinetics of photocatalysis.

3.2.5. Kinetics of Photocatalysis

The kinetics of heterogeneous photocatalysis obey the Langmuir–Hinshelwood model. If the initial concentration of the dye is low, the model could be simplified to a pseudo-first order equation [16,28,29]:

$$\ln\left(\frac{c}{c_0}\right) = -k_{app}t \quad (2)$$

where c_0 is the initial dye concentration (mg/L), c is the concentration of the dye at time t (mg/L), t is the irradiation time (min) and k_{app} is the apparent rate constant (min^{-1}).

The representations of $-\ln(c/c_0)$ as a function of time are presented as insets in Figures 7 and 8, which present the experimental results obtained in different initial condi-

tions of photocatalysis. In Table 2 are given the calculated values of the constant k_{app} for the presented experiments. It could be noticed that the kinetic constants are higher when material EthylAmAcid is utilized as a photocatalyst.

3.2.6. Structural Changes in CR Molecule during Photocatalysis

By analyzing the changes that occur in the UV-VIS spectra of the CR solution during the photocatalysis test, information can be obtained about the structural changes in the dye molecule following the oxidation process.

Figure 9a shows the UV-VIS spectra of the 50 mg/L CR solution subjected to photocatalysis with 1 g/L material EthylAmAcid. The CR dye solution has three absorption bands in the UV-VIS spectrum. The absorption band with the maximum at 498 nm is due to the azo bond and the decrease in the intensity of this band corresponds to the break of this bond, so it corresponds to the discoloration of the solution. The other two absorption bands in the UV domain, with maxima at 340 nm and 235 nm, are due to the benzene and naphthalene rings, respectively. The decrease in intensity of these bands is due to the opening of the naphthalene and benzene aromatic rings, with the formation of intermediate products. During the photocatalysis process, the maxima of the absorption bands decrease in intensity, without any shifting taking place since probably the CR oxidation products do not absorb UV-VIS radiation. After 240 min, the spectrum of the CR solution became almost flat, because of the opening of the benzene and naphthalene rings and the breaking of the azo bonds from the dye molecules.

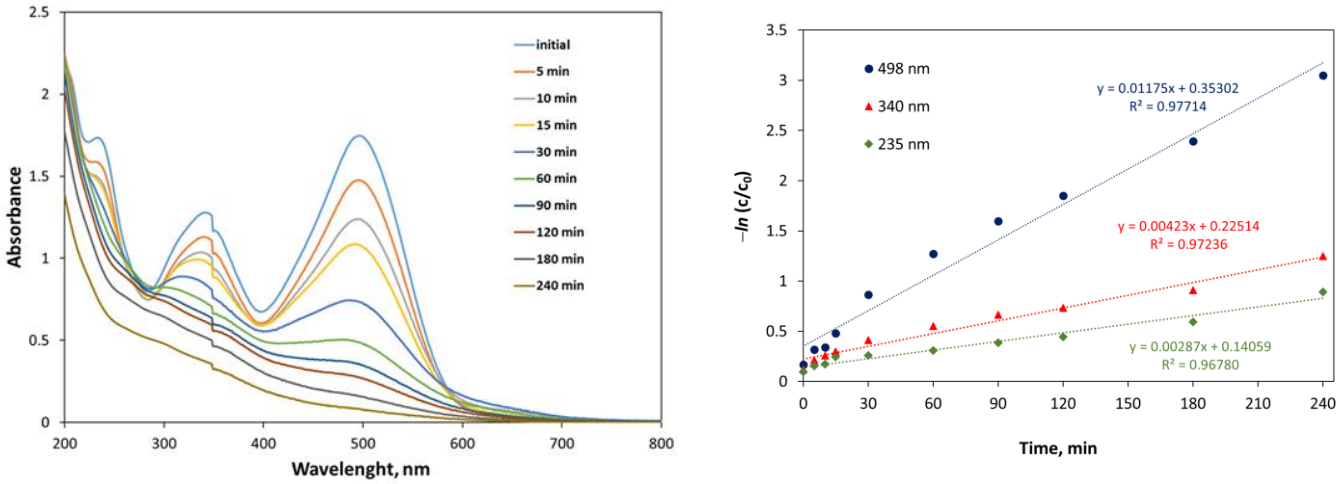

(**a**) (**b**)

Figure 9. UV-VIS spectra of 50 mg/L CR solution during the photocatalytic test with 1 g/L EthylAmAcid as the photocatalyst (**a**); kinetic model for the dye discoloration: naphthalene ring opening and benzene ring opening (**b**).

By applying the pseudo-first order kinetic model for the three absorption peaks, information can be obtained on the rates of discoloration and the opening of naphthalene and benzene rings (Figure 9b). The fastest process is discoloration, the breaking of the azo bonds having the rate constant $k_{app} = 1.18 \times 10^{-2}$ min^{-1}. Following this occurs the breaking of the naphthalene rings, with $k_{app} = 4.23 \times 10^{-3}$ min^{-1}, then the breaking of the benzene rings, with the rate constant $k_{app} = 2.87 \times 10^{-3}$ min^{-1}.

3.2.7. Reusability of the Catalysts

In order to evaluate the possibility of catalyst reuse, three cycles of CR degradation were performed. After each experiment, the catalyst was separated by filtration from the dye solution, washed with distilled water and dried at 105 °C overnight. Figure 10 shows

the efficiency of CR degradation by reusing the photocatalysts. The tests were conducted by using the conditions in which the photodegradation efficiency in the first cycle was maximum: 25 mg/L CR solution with 1 g/L EthylAmAcid and 50 mg/L CR solution with 2 g/L BenzylAmAcid. Both catalysts showed good stability when reused, the efficiency of heterogeneous photocatalysis remaining higher than 90% even after three cycles.

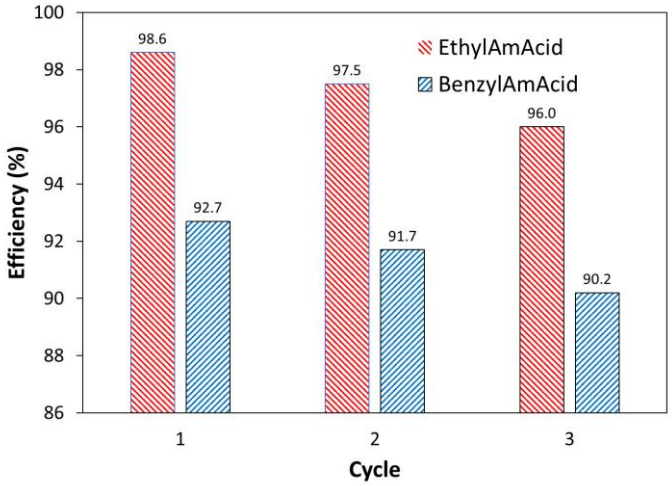

Figure 10. Reusability of the catalysts.

Table 3 presents the performance of various photocatalysts, mentioned in the specialtist literature, developed in the treatment process of water with CR content. It could be observed that the synthesized materials present a superior efficiency compared with more expensive and difficult to synthesize inorganic or organic nanoparticles and composites, which achieved a lower degradation efficiency, needing a much higher treatment time and using a lower initial concentration of the CR in the solution.

Table 3. CR photocatalysis by using different materials.

Material	c_0 (mg/L)	Solid:Liquid (g/L)	Time (min)	Efficiency (%)	Ref
Mg-TiO_2 nanoparticles	17	0.5	420	80	[30]
TiO_2 nanoparticles	55	1	480	90	[31]
$CoFe_2O_4$	5	-	90	90	[32]
PANi/BiOCl	10	1	60	88.4	[33]
EthylAmAcid	25	1	240	98.6	This study
BenzylAmAcid	50	2	240	92.7	This study

4. Conclusions

In the present study, two novel compounds of β-phosphonate-type glycine pendant groups grafted on S-DVB copolymer were synthetized by utilizing the one-pot synthesis procedure. The synthesized materials were characterized by FTIR spectroscopy, scanning electron microscopy, EDX spectroscopy, thermogravimetric analysis and UV-VIS spectroscopy. The use of synthesized materials together with aldehyde support as catalysts in the heterogeneous photocatalysis of Congo red dye showed that grafting of the support results in increased efficiency of the process. Material EthylAmAcid had, under all experimental conditions, a better efficiency of dye removal than material BenzylAmAcid. The initial concentration of the dye and the solid material content influence the oxidation efficiency of CR. The kinetics of the process follow a model of pseudo-first order. UV-VIS spectra of the dye solution show that during photocatalysis, the first process is to break the azo bonds, and then the breaking of the naphthalene and benzene rings takes place.

Author Contributions: Conceptualization, A.P. (Adriana Popa) and L.C.; methodology, A.V.; formal analysis, L.L. and A.P. (Aniela Pop); investigation, L.L., A.P. (Adriana Popa), L.C. and A.P. (Aniela Pop); writing—original draft preparation, A.P. (Adriana Popa) and L.C.; writing—review and editing, L.L. and L.C.; visualization, A.P. (Adriana Popa); supervision, A.V. All authors have read and agreed to the published version of the manuscript.

Funding: This research received no external funding.

Institutional Review Board Statement: Not applicable.

Informed Consent Statement: Not applicable.

Data Availability Statement: Data are contained within the article.

Conflicts of Interest: The authors declare no conflict of interest.

References

1. Nasar, A.; Mashkoor, F. Application of polyaniline-based adsorbents for dye removal from water and wastewater—A review. *Environ. Sci. Pollut. Res.* **2019**, *26*, 5333–5356. [CrossRef] [PubMed]
2. Tkaczyk, A.; Mitrowska, K.; Posyniak, A. Synthetic organic dyes as contaminants of the aquatic environment and their implications for ecosystems: A review. *Sci. Total Environ.* **2020**, *717*, 137222. [CrossRef] [PubMed]
3. Kant, R. Textile dyeing industry an environmental hazard. *Nat. Sci.* **2012**, *4*, 22–26. [CrossRef]
4. Holkar, C.R.; Jadhav, A.J.; Pinjari, D.V.; Mahamuni, N.M.; Pandit, A.B. A critical review on textile wastewater treatments: Possible approaches. *J. Environ. Manag.* **2016**, *182*, 351–366. [CrossRef]
5. Adane, T.; Adugna, A.T.; Alemayehu, E. Textile Industry Effluent Treatment Techniques. *J. Chem.* **2021**, *2021*, 5314404. [CrossRef]
6. Mirza, N.R.; Huang, R.; Du, E.; Peng, M.; Pan, Z.; Ding, H.; Shan, G.; Ling, L.; Xie, Z. A review of the textile wastewater treatment technologies with special focus on advanced oxidation processes (AOPs), membrane separation and integrated AOP-membrane processes. *Desalination Water Treat.* **2020**, *206*, 83–107. [CrossRef]
7. Maranescu, B.; Lupa, L.; Visa, A. Heavy metal removal from waste waters by phosphonate metal organic frameworks. *Pure Appl. Chem.* **2018**, *90*, 35–47. [CrossRef]
8. Lupa, L.; Maranescu, B.; Visa, A. Equilibrium and kinetic studies of chromium ions adsorption on Co(II) based phosphonate metal organic frameworks. *Sep. Sci. Technol.* **2018**, *53*, 1017–1026. [CrossRef]
9. Miklos, D.B.; Remy, C.; Jekel, M.; Linden, K.G.; Drewes, J.E.; Hübner, U. Evaluation of advanced oxidation processes for water and wastewater treatment—A critical review. *Water Res.* **2018**, *139*, 118–131. [CrossRef]
10. Bolton, J.R.; Bircher, K.G.; Tumas, W.; Tolman, C.A. Figures-of-merit for the technical development and application of advanced oxidation technologies for both electric- and solar-driven systems (IUPAC Technical Report). *Pure Appl. Chem.* **2001**, *73*, 627–637. [CrossRef]
11. Thota, S.; Tirukkovalluri, S.R.; Bojja, S. Visible light induced photocatalytic degradation of methyl red with codoped titania. *J. Catal.* **2014**, *2014*, 962419. [CrossRef]
12. Andronic, L.; Isac, L.; Cazan, C.; Enesca, A. Simultaneous Adsorption and Photocatalysis Processes Based on Ternary TiO_2–Cu_xS–Fly Ash Hetero-Structures. *Appl. Sci.* **2020**, *10*, 8070. [CrossRef]
13. Dvininov, E.; Popovici, E.; Pode, R.; Cocheci, L.; Barvinschi, P.; Nica, V. Synthesis and characterization of TiO_2-pillared Romanian clay and their application for azoic dyes photodegradation. *J. Hazard. Mater.* **2009**, *167*, 1050–1056. [CrossRef]
14. Velmurugan, R.; Swaminathan, M. An efficient nanostructured ZnO for dye sensitized degradation of reactive red 120 dye under solar light. *Sol. Energ. Mat. Sol. C* **2011**, *95*, 942–950. [CrossRef]
15. Salem, I.A.; El-Ghamry, H.A.; El-Ghobashy, M.A. Catalytic decolorization of Acid blue 29 dye by H_2O_2 and a heterogeneous catalyst. *Beni-Suef Univ. J. Basic Appl. Sci.* **2014**, *3*, 186–192. [CrossRef]
16. Golban, A.; Cocheci, L.; Lazau, R.; Lupa, L.; Pode, R. Iron ions reclaiming from sludge resulted from hot-dip galvanizing process, as Mg_3 Fe-layered double hydroxide used in the degradation process of organic dyes. *Desalination Water Treat.* **2018**, *131*, 317–327. [CrossRef]
17. Sarkar, S.; Ponce, N.T.; Banerjee, A.; Bandopadhyay, R.; Rajendran, S.; Lichtfouse, E. Green polymeric nanomaterials for the photocatalytic degradation of dyes: A review. *Environ. Chem. Lett.* **2020**, *18*, 1569–1580. [CrossRef]
18. Orooji, Y.; Akbari, R.; Nezafat, Z.; Nasrollahzadeh, M.; Kamali, T.A. Recent signs of progress in polymer-supported silver complexes/nanoparticles for remediation of environmental pollutants. *J. Mol. Liq.* **2021**, *329*, 115583. [CrossRef]
19. Shilpa, E.R.; Gayathri, V. Polymer immobilized Fe(III) complex of 2-phenylbenzimidazole: An efficient catalyst for photodegradation of dyes under UV/Visible light irradiation. *J. Saudi Chem. Soc.* **2018**, *22*, 678–691. [CrossRef]
20. Davidescu, C.M.; Ardelean, R.; Popa, A. Performance of poly(styrene-co-divinylbenzene) functionalized with different aminophosphonate pendant groups, in the removal of phenolic compounds from aqueous solutions. *Pure Appl. Chem.* **2016**, *88*, 993–1004. [CrossRef]
21. Popa, A.; Ene, R.; Visinescu, D.; Dragan, E.S.; Ilia, G.; Iliescu, S.; Parvulescu, V. Transitional metals immobilized by coordination on aminophosphonate functionalized copolymers and their catalytic properties. *J. Mol. Catal. A-Chem.* **2015**, *408*, 262–270. [CrossRef]

22. Amin, P.O.; Ketuly, K.A.; Saeed, S.R.; Muhammadsharif, F.F.; Symes, M.D.; Paul, A.; Sulaiman, K. Synthesis, spectroscopic, electrochemical and photophysical properties of high band gap polymers for potential applications in semi-transparent solar cells. *BMC Chem.* **2021**, *15*, 25. [CrossRef] [PubMed]
23. Cocheci, L.; Lupa, L.; Pop, A.; Visa, A.; Maranescu, B.; Popa, A. Photocatalytical degradation of Congo red azo dye using phosphono-aminoacid-Cd(II) pendant groups grafted on a polymeric support. *Rev. Chim.-Buchar.* **2019**, *70*, 3473–3476. [CrossRef]
24. Chen, J.; Xiong, Y.; Duan, M.; Li, X.; Li, J.; Fang, S.; Qin, S.; Zhang, R. Insight into the synergistic effect of adsorption–photocatalysis for the removal of organic dye pollutants by Cr-doped ZnO. *Langmuir* **2020**, *36*, 520–533. [CrossRef] [PubMed]
25. Feng, J.; Ran, X.; Wang, L.; Xiao, B.; Lei, L.; Zhu, L.; Liu, Z.; Xi, X.; Feng, G.; Dai, Z.; et al. The synergistic effect of adsorption-photocatalysis for removal of organic pollutants on mesoporous Cu2V2O7/Cu3V2O8/g-C3N4 heterojunction. *Int. J. Mol. Sci.* **2022**, *23*, 14264. [CrossRef] [PubMed]
26. Singh, S.; Perween, S.; Ranjan, A. Dramatic enhancement in adsorption of congo red dye in polymer-nanoparticle composite of polyaniline-zinc titanate. *J. Environ. Chem. Eng.* **2021**, *9*, 105149. [CrossRef]
27. Chen, Y.; Chen, S.; Deng, Z.; Xu, X.; Qin, J.; Guo, X.; Bai, Z.; Chen, X.; Lu, Z. Fabrication of polystyrene/CuO@calcined layered double hydroxide microspheres with high adsorption capacity for Congo red. *Colloid. Surf. A* **2022**, *652*, 129827. [CrossRef]
28. Asenjo, N.G.; Santamaria, R.; Blanco, C.; Granda, M.; Alvarez, P.; Menendez, R. Correct use of the Langmuir–Hinshelwood equation for proving the absence of a synergy effect in the photocatalytic degradation of phenol on a suspended mixture of titania and activated carbon. *Carbon* **2013**, *55*, 62–69. [CrossRef]
29. Nguyen, C.H.; Tran, H.N.; Fu, C.C.; Lu, Y.T.; Juang, R.S. Roles of adsorption and photocatalysis in removing organic pollutants from water by activated carbon-supported titania composites: Kinetic aspects. *J. Taiwan Inst. Chem. E* **2020**, *109*, 51–61. [CrossRef]
30. Bhagwat, U.O.; Wu, J.J.; Asiri, A.M.; Anandan, S. Sonochemical Synthesis of Mg-TiO_2 nanoparticles for persistent Congo red dye degradation. *J. Photochem. Photobiol. A* **2017**, *346*, 559–569. [CrossRef]
31. Ćurković, L.; Ljubas, D.; Juretic, H. Photocatalytic decolorization kinetics of diazo dye Congo Red aqueous solution by UV/TiO_2 nanoparticles. *React. Kinet. Mech. Catal.* **2010**, *99*, 201–208. [CrossRef]
32. Ali, N.; Said, A.; Ali, F.; Raziq, F.; Ali, Z.; Bilal, M.; Reinert, L.; Begum, T.; Iqbal, H.M.N. Photocatalytic degradation of Congo red dye from aqueous environment using cobalt ferrite nanostructures: Development, characterization, and photocatalytic performance. *Water Air Soil Pollut.* **2020**, *231*, 50. [CrossRef]
33. Namdarian, A.; Tabrizi, A.G.; Arsalani, N.; Khataee, A.; Mohammadi, A. Synthesis of PANi nanoarrays anchored on 2D BiOCl nanoplates for photodegradation of Congo Red in visible light region. *J. Ind. Eng. Chem.* **2020**, *81*, 228–236. [CrossRef]